

Electronic transport properties of BN sheet on adsorption of ammonia (NH₃) gas

Anurag Srivastava · Chetan Bhat · Sumit Kumar Jain ·
Pankaj Kumar Mishra · Ranjeet Brajpuriya

Received: 2 July 2014 / Accepted: 26 January 2015
© Springer-Verlag Berlin Heidelberg 2015

Abstract We report the detection of ammonia gas through electronic and transport properties analysis of boron nitride sheet. The density functional theory (DFT) based ab initio approach has been used to calculate the electronic and transport properties of BN sheet in presence of ammonia gas. Analysis confirms that the band gap of the sheet increases due to presence of ammonia. Out of different positions, the bridge site is the most favorable position for adsorption of ammonia and the mechanism of interaction falls between weak electrostatic interaction and chemisorption. On relaxation, change in the bond angles of the ammonia molecule in various configurations has been reported with the distance between NH₃ and the sheet. An increase in the transmission of electrons has been observed on increasing the bias voltage and I-V relationship. This confirms that, the current increases on applying the bias when ammonia is introduced while a very small current flows for pure BN sheet.

Keywords Ab initio · Ammonia · Band structure · Boron Nitride · I-V · Sensor

Introduction

Geim and Novoselov in 2004 isolated a single sheet of graphite, which later became popular as graphene. This two dimensional structure has a sp² hybridized form of carbon with hexagonal geometry, having C–C bond length of 1.42 Å [1, 2]. Graphene has excellent electrical, mechanical, and optical properties and hence wide areas of applications are possible [3, 4]. This graphene sheet with a zero band gap semiconductor hinders the application of graphene sheet in the field of electronics, however, by functionalization, the band gap can be introduced and in turn increases possibility of graphene based devices [4–6]. One-dimensional (1D) boron nitride nanotube (BNNT) and 2D hexagonal BN (h-BN) are attractive for demonstrating fundamental physics and promising applications in nano-/microscale devices. However, there is a high anisotropy associated with these BN allotropes as their excellent properties are either along the tube axis or in-plane directions, posing an obstacle in their widespread use in technological and industrial applications. Recently, Sakhavand and Shahsavari [7] have reported a series of 3D BN prototypes, namely, pillared boron nitride (PBN), by fusing single-wall BNNT and monolayer h-BN with an aim to fill this gap. However, in 2005, an identical nanosheet having similar geometry as of graphene viz. boron nitride sheet (BN) has been derived, with a band gap in the range of 4.2–6 eV [8–10], which has remarkably been accepted as a material with modified and magnificent properties for application in the field of optoelectronics and sensors [11–13].

Recently, gas sensing has come out as a field of continuous research, detection of toxic gas is of utmost importance as lives of living beings is at stake [14–17]. Even a very small leakage of toxic gas in industries, power plants, domestic homes, and environment can cause hazardous effects, which ultimately lead to death. Therefore, detection of toxic gas is of significant importance. Ammonia gas is used in industries,

A. Srivastava (✉) · C. Bhat · S. K. Jain
Advanced Material Research Group, CNT Lab, ABV-IIITM,
Gwalior, M.P., India
e-mail: profanurag@gmail.com

C. Bhat
Amity School of Engineering Technology, Amity University,
Haryana, India

P. K. Mishra
Amity School of Applied Science Amity University, Gwalior, M.P.,
India

R. Brajpuriya
Amity School of Applied Science, Amity University, Haryana, India

food processing units, refrigeration and fertilisers etc. Exposure to ammonia leads to respiratory problems, irritation in eyes and damage to human skin. Concentration of ammonia even at dilute levels is highly toxic for the aquatic animals, for this reason it is being classified as a dangerous gas for the environment. Different types of sensing mechanisms have been designed for the detection of ammonia, e.g., metal oxide sensors, catalytic sensors, etc. [15–17]. The aim of this paper is to investigate the effect of the presence of the ammonia molecule near the boron nitride sheet (BN sheet) and interrogate the quality of interaction. It is well known that the adsorption has two different approaches governed by weak electrostatic interaction (physisorption) [18, 19] and comparative strong interaction by charge dispersion interaction (chemisorption) [20, 21]. Our group has recently reported the electronic and transport properties of silicene and germanene [22], nanoribbons [23, 24], and nanotubes [25] by using DFT based ab initio approach. In view of remarkable features of the BN sheet and need of ammonia detection, we thought it pertinent to explore the possibility of analysing the boron nitride sheet (BN sheet) as a sensing material to track down the effect of ammonia exposure.

Computational methods

The calculations are performed by using density functional theory (DFT) [26, 27] based Atomistix virtual nano lab (ATK-VNL) [28] tool. The optimizations were performed using generalized gradient approximation (GGA) [29, 30] as exchange–correlation functional, with revised Perdew, Burke, and Ernzerof (revPBE) [31] type parameterization. The structures were relaxed using a double zeta double polarized type of basis sets with an energy mesh cut-off of 75 Hartree and $1 \times 13 \times 13$ k-point and maximum force tolerance of 0.0001 eV/Å. It has been attempted to get the gas molecule attached to the BN sheet at different locations to check for better sensitivity. For transport properties, a two probe model has been devised for ammonia detection by analyzing its conductance.

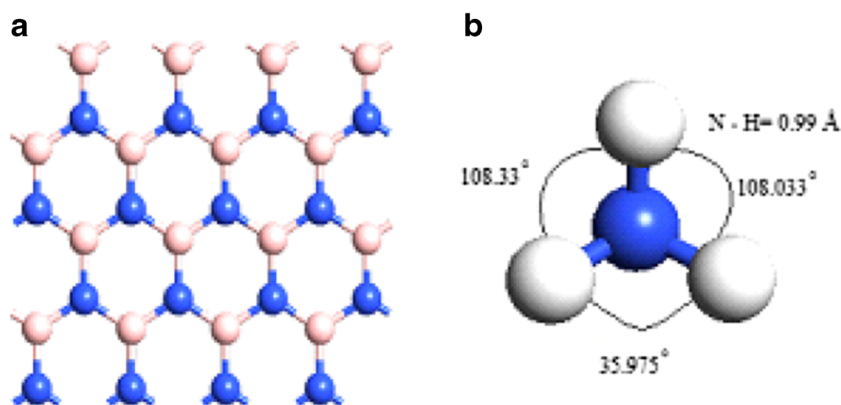
Results and discussion

In the present piece of work, a BN sheet with width $n=8$ has been analyzed in the presence of an ammonia gas (NH_3) molecule present at different sites of the BN sheet. The sheet used in the calculation contains 16 boron and 16 nitrogen atoms for boron nitride sheet, without any functionalization (Fig. 1a). The effect on the BN sheet on exposure of a single molecule of NH_3 (Fig. 1b) has been investigated by analyzing its electronic and transport properties. Also, various positions have been tested and analyzed to determine the adsorption of the NH_3 molecule on the BN sheet. Different geometries of the BN sheet with ammonia (NH_3) used for the present work are given in Fig. 2. Four positions of ammonia gas molecule have been considered: (a) on the center of the hexagon and perpendicular to the sheet (Fig. 2a), (b) on the bridge site (Fig. 2b), (c) top of the sheet and perpendicular to boron atom (Fig. 2c), and (d) top of the sheet and perpendicular to nitrogen atom (Fig. 2d).

The stability of BN sheet has been analyzed in terms of total energy and binding energy computation for different sites of the ammonia molecule presence, tabulated in Table 1, confirms that the bridge site is more stable. Total energy and adsorption energy has been calculated for the above mentioned systems, with different sites of the ammonia molecule on BN sheet. The calculated adsorption energies for the different configurations are in the range of -0.436 to -0.53 eV. The negative adsorption energy for these configurations corresponds to an exothermic reaction and hence energetically favorable. It is also observed that the bridge site with highest adsorption energy and minimum total energy is the best site for adsorption of ammonia gas as depicted in Fig. 2(b). The competitions between relatively large distance and significant binding energy of NH_3 from the BN surface are further scrutinized in terms of density of state (DOS) analysis.

The relaxed structures for all the geometries with change in the bond lengths and the bond angles are shown in Fig. 3(a–d), where, it is observed that for all the positions, NH_3 molecule

Fig. 1 Initial structure of (a) pristine BN sheet and (b) ammonia molecule



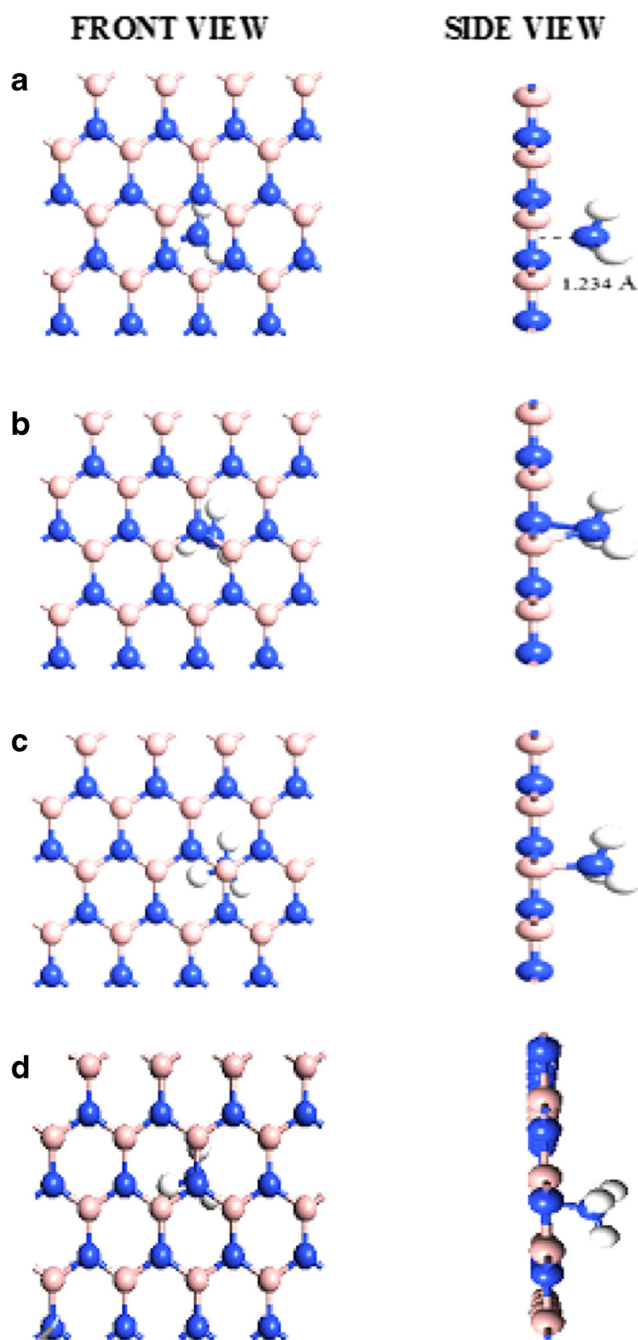


Fig. 2 Front view and side view of initial positions of NH_3 molecule positioned (a) at the center of hexagon, b on the bridge site, c on the top of boron atom and (d) on the top of nitrogen atom of the BN sheet

Table 1 Total energy and binding energy of BN sheet

Position of NH_3 molecule	Total energy(eV)	Binding energy(eV)
Center	-5988.79	0.48
Bridge site	-5988.88	0.39
N-BN	-5988.79	0.48
B-BN	-5988.87	0.40

prefers different orientations. Initially, the ammonia molecule is placed at a distance of 1.23 Å from the surface of the BN sheet and after relaxation. The separation of NH_3 and BN sheet has further changed to 3.97, 3.317, 3.383, and 3.863 Å respectively, for positions (a)–(d). Maximum separation is observed when the NH_3 molecule is placed at the bridge site (Fig. 3a) while minimum when placed at the center of the hexagon (Fig. 3b). NH_3 molecule oriented with 'N' atom pointing toward the BN sheet, for bridge site and top site perpendicular to boron atom, shown in Fig. 3b and c, however, all the three hydrogen atoms of NH_3 gas molecule point toward the BN sheet with 'N' atom moving away for position a and d shown in Fig. 3a and d.

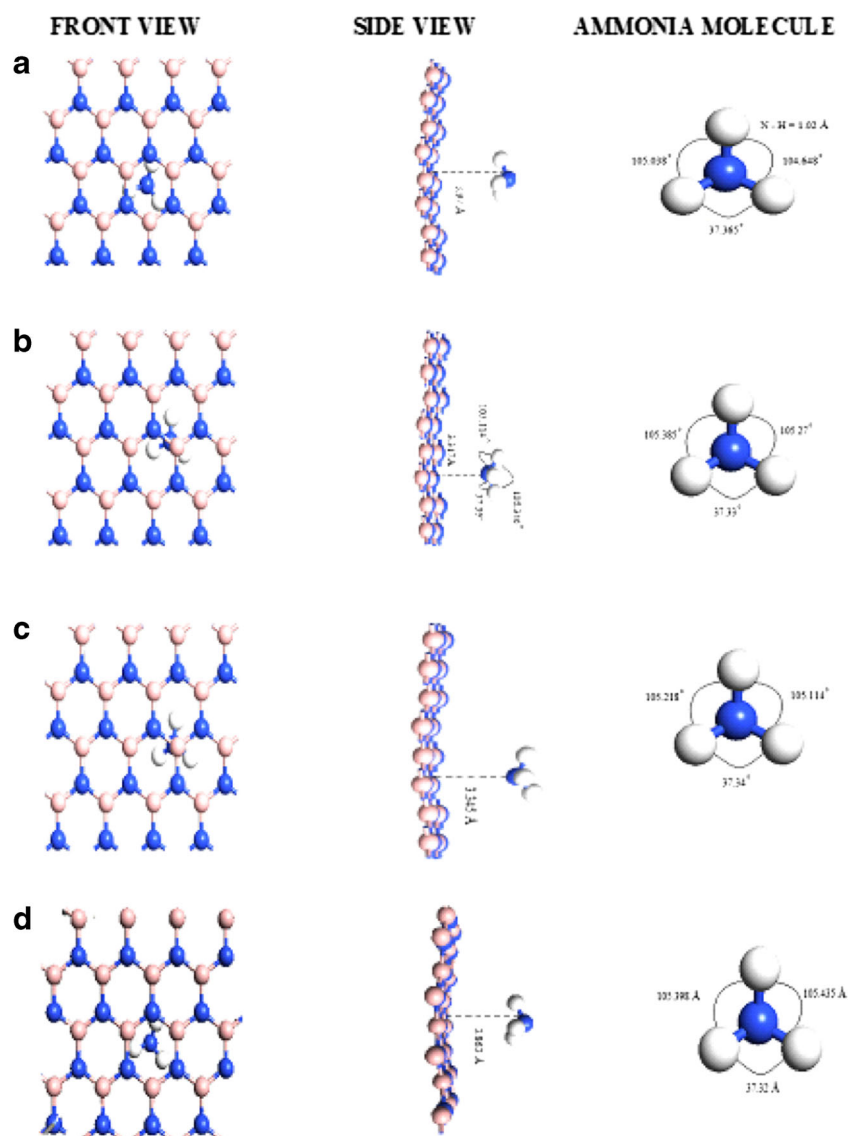
The orientation of the NH_3 molecule for various adsorption sites is also shown in Fig. 3. A significant change in the bond angles of the NH_3 molecule is observed. The N-H bond length for ammonia molecule is 0.997 Å (Fig. 1b), which on optimization changes to 1.02 Å. Computation also shows that the bond angle for a simple gas molecule H-N-H orient to 105.435, 105.398, and 37.32°. On optimization, the orientation alters to

- 105.385, 105.27, and 37.33 for center of hexagon.
- 105.038, 104.648, and 37.365 for bridge site.
- 105.218, 105.114, and 37.34 for top site of B atom.
- 105.398, 105.435, and 37.34 for top site of nitrogen atom.

Electronic properties

The electronic properties of relaxed geometry of BN sheet for various positions of the NH_3 gas molecule on it have been investigated through band structure and density of states analysis for each structure presented in Fig. 4. The band structure of a pristine BN sheet shows that no energy level crosses the zero level or Fermi level and the evaluated band gap is 4.601 eV (Fig. 4a), confirms this as a wide band gap semiconductor. Band gap or energy gap is defined as the difference between the highest occupied molecular orbital and lowest unoccupied molecular orbital (HOMO-LUMO). This is in line with the others reports [8–11], illustrating the fact that the band gap for BN sheet is in the range of 4.5–6 eV. It is also seen that on introduction of the ammonia molecule on the surface of the BN sheet, this band gap increases. Total energy and adsorption energy calculation confirms that the bridge site is the most favorable for the adsorption of NH_3 on BN sheet, hence for further computations, the bridge site of the NH_3 molecule has been preferred. On placing the NH_3 molecule at the bridge site, energy gap increases to 4.753 eV (Fig. 4c). For all other configurations, almost the same band gap has been observed.

Fig. 3 Front view and side view of optimized structure of BN sheet with NH_3 molecule (**a**) at the center of hexagon, **b** on the bridge site, **c** on the top of boron atom, and (**d**) on the top of the nitrogen atom of the BN sheet



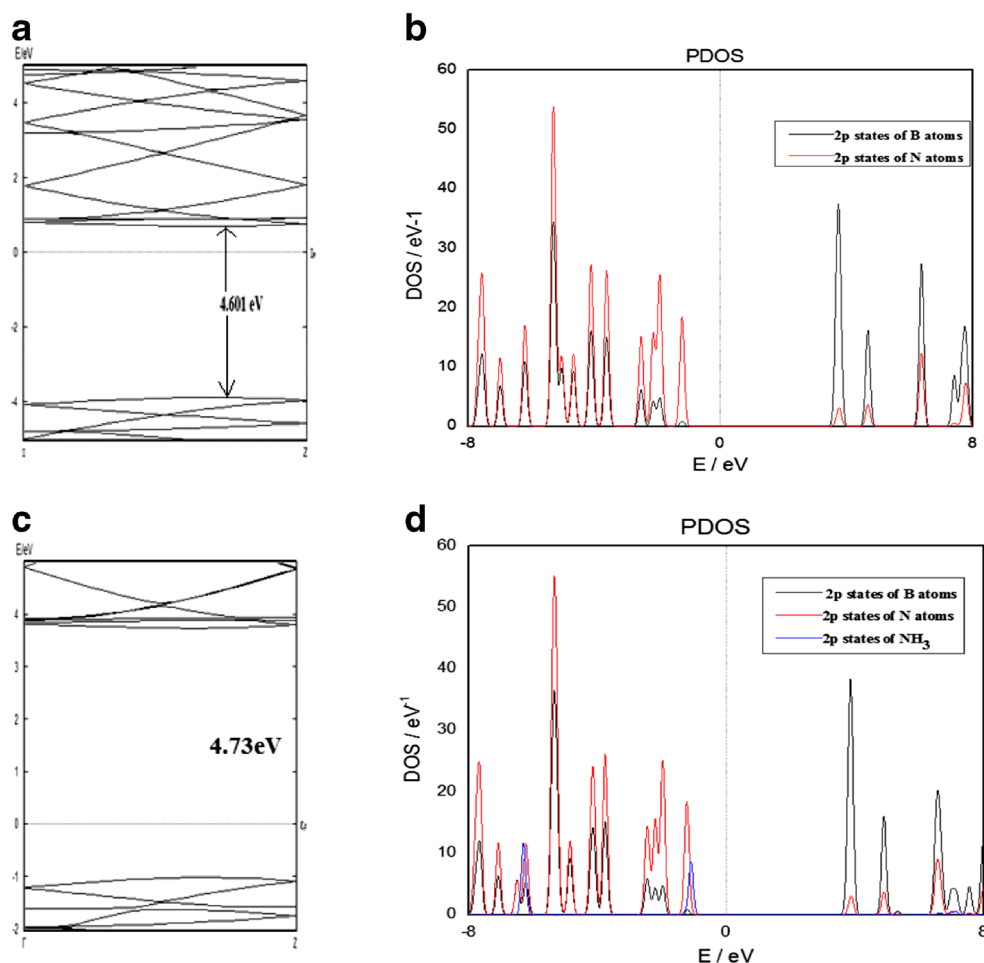
To further analyze the electronic properties of the structures, partial density of states (PDOS) have also been investigated and shown in Fig. 4b and d, represents the number of electronic states available for occupancy per energy level. Here, it is observed that no electronic states are present at the Fermi level, validates the wide band semiconducting behavior of BN sheet. PDOS analysis of a pristine BN sheet shows that in upper valence band, the 2p states of N atoms dominate, with the maximum peak of 53.3 at 5.24 eV, few electronic states are present near the Fermi level, and however, there is no significant impact in the conduction band. On the contrary, 2p states of B atoms show their dominance in the conduction band with a maximum peak of 36.5 at 4.24 eV. Figure 4(d) depicts the PDOS of NH_3 positioned at bridge site, where, it can be seen that there is an increase in the band gap; however no states are present at the Fermi level and 2p states of N atoms of ammonia gas molecule show their presence in

the valence band and near to Fermi level. From Fig. 4(d) it can be examined that there is no significant interaction between the p orbital of NH_3 and the π -bonding orbital of BN sheet except a feeble interaction near HOMO region and at the innermost occupied orbital. As a consequence it could be interpreted that adsorption of ammonia to BN surface falls under the intermediate of chemisorption and weak electrostatic interaction.

Transport properties

For better understanding the presence of NH_3 on the BN sheet and validating the electronic properties discussed in an earlier section, it is worth examining the I-V characteristics. For which a two probe system has been modeled using optimized (2, 2) pristine BN sheet, shown in Fig. 5a. This two probe

Fig. 4 Band structure and density of states (DOS) of pristine BN sheet (a) and (b), NH_3 gas molecule positioned at the bridge site of a BN sheet (c) and (d)

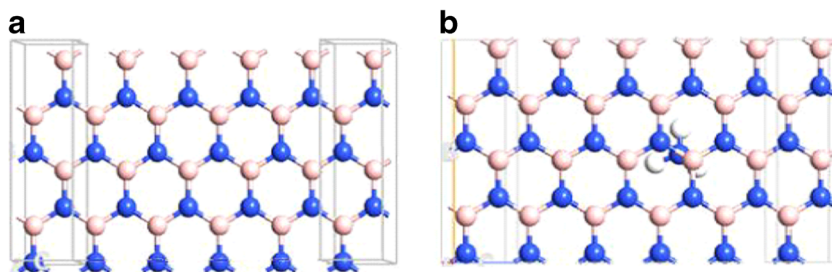


model has three parts, left electrode, right electrode, and central region. Where, central region constitutes scattering region, left and right electrode extensions [32–34]. A large K point sampling of $1 \times 1 \times 100$ has been found suitable to calculate the transmission spectrum and I-V relationship. For this purpose, Landauer based approach is used to describe the transport at microscopic level. This approach defines the electric current through a material in terms of probability of the electron to pass through it, called transmission probability $T(E)$.

In transport properties, the electric current has been calculated by using the Landauer formula [30–32]:

$$I = T(E)[f_L(E) - f_R(E)]dE,$$

Fig. 5 Two probe model of (a) pristine BN sheet and (b) NH_3 at the bridge site, for calculation of transmission spectrum and I-V relationship



where $f_L(E)$ and $f_R(E)$ are the Fermi level distribution for left and right electrode and $T(E)$ is the transmission probability, written as:

$$T(E) = T_r(\Gamma_L(E, V)G^R(E, V)\Gamma_R(E, V)G^A(E, V)),$$

where $\Gamma_{L,R}$ are the coupling functions and G^R and G^A retarded and advanced greens function of the conductor [35, 36]. The current is proportional to the conductance G , evaluated at the Fermi level of the device. The transport properties of the following configurations have been analyzed on applying the bias voltage of -2 to 2 V and shown in Fig. 5a and b. Here,

Fig. 6 Projected density of states and transmission spectrum for (a) pristine BN sheet device, and (b) NH_3 introduced at the bridge site

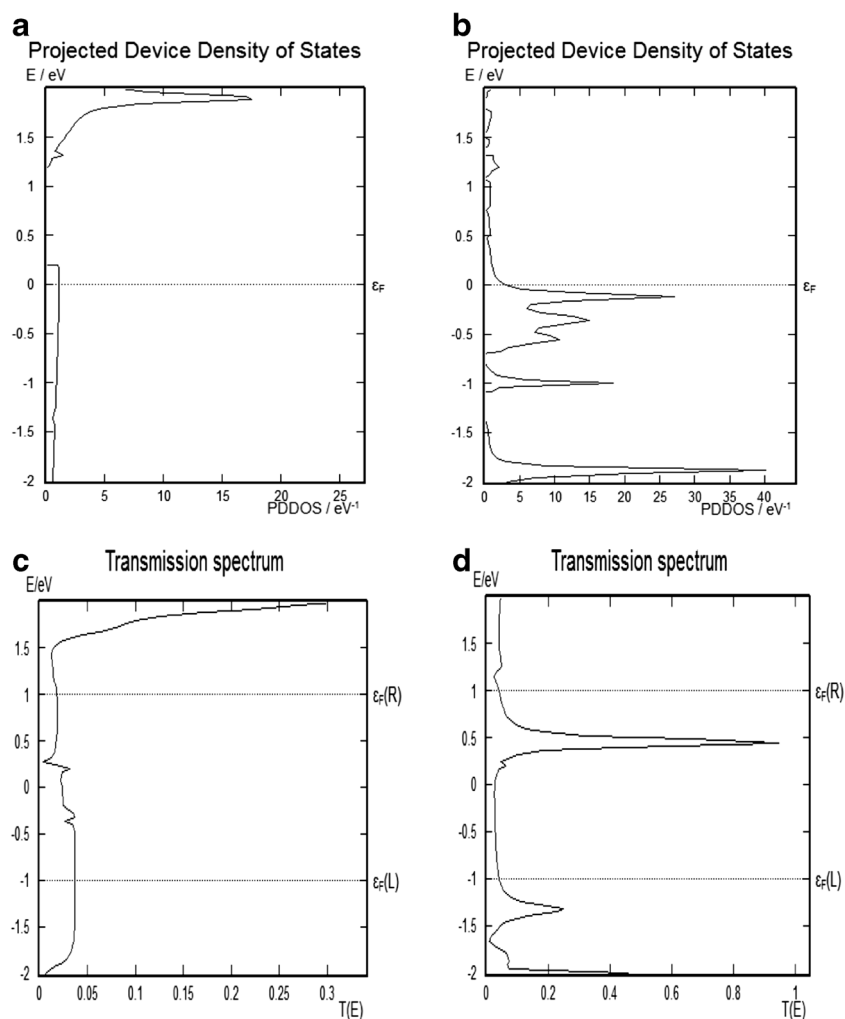


Fig. 5a shows a device for a pristine BN sheet while Fig. 5b represents the device for NH_3 placed at the most favorable bridge site of the sheet.

The device density of states (DDOS) and transmission spectrum are shown in Fig. 6. The DDOS of pristine sheet

shows a negligible number of energy states present at the Fermi level. The maximum number of energy levels to be occupied by the electrons for conduction is at 1.88 eV with the peak of 16.5 eV in the upper part of the conduction band. While for the bridge site, highest peak of 40 eV is seen at the top of the valance band near the Fermi level, at 1.9 eV. This shows that the possibility of electrons occupying states close to the Fermi level has increased.

The transmission spectrum is shown in Fig. 6c and d, where the possibility of the number of transmitted electrons

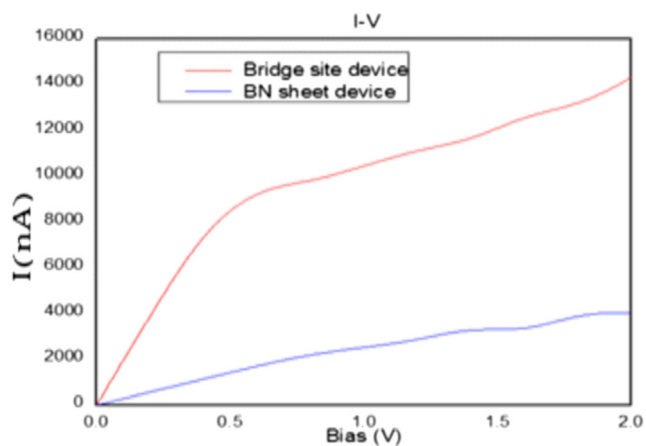


Fig. 7 I-V characteristics of pristine BN sheet and NH_3 at bridge site of the molecule

Table 2 Charge transfer due to NH_3 molecule near the BN sheet in terms of Mulliken population

NH_3 position	Mulliken population of NH_3	Charge transferred from NH_3 to BN sheet
NH_3 (in bridgesite)	7.952	0.048
NH_3 (in N- NH_3)	7.992	0.008
NH_3 (in NH_3 @boron)	7.952	0.048
NH_3 (in NH_3 @center)	7.991	0.009

is observed on applying the bias. In the case of no bias, the transmission of electrons in the valence as well as conduction energy levels does not take place and the net current is zero. However, on applying the bias, the electrons gain velocity and the bond breaks and that results in a peak. For the pure BN sheet, the transmission coefficient at Fermi level is approximately zero, which agrees with our electronic band structure. However maximum transmission of electrons is observed in the upper part of the Fermi level at 2 eV with a peak of 0.3 eV. Figure 6(b) shows that for NH_3 adsorbed BN sheet transmission of electrons is maximum at 0.4 eV and the transmission coefficient increased to 0.95. To analyze this effect, we applied the bias on electrode in the range of -2 to 2 V shown in I-V curve (Fig. 7), which gives the relationship between the current and the voltage.

The current–voltage characteristics of the pristine BN sheet show that when bias is applied, no current flows through the device, while on increasing the voltage, a very small increase in the current has been observed. Even when voltage up to 2 V is applied, a very small current passes through the device and the maximum current flowing through the pristine BN sheet device is $3 \mu\text{A}$ and does not show a linear relationship. On the contrast, when a device that is constructed through optimized BN sheet with NH_3 at bridge site, shows an approximate linear relationship between the current and bias voltage till 0.4 V and a maximum current of $14.05 \mu\text{A}$ is observed at 1.94 V. This increase in current with bias voltage may be due to the fact that on increasing the bias, the DDOS and the transmission spectrum show the presence of few electronic states near the Fermi level for bridge site configuration.

The above discussion confirms the sensing ability of BN sheet analyzed in terms of comparative electronic band structure and transmission spectrums of pristine BN sheet and with presence of NH_3 molecule.

Charge transfer analysis

To analyze further the presence of ammonia near the BN sheet surface, we have computed the Mulliken population for each individual atom and material which are included in the analysis of this paper. Mulliken population of an element is nothing but its number of valence electrons; similarly for a material it is the sum of the valence electrons of each atom of that material. In the present work, atomic number of boron is 5 ($1s^2 2s^2 2p^1$), whereas the valence electrons are only 3 ; so the Mulliken population of isolated boron is 3 . Similarly for the NH_3 , it has one nitrogen and three hydrogen atoms, where, an isolated nitrogen ($1s^2 2s^2 2p^3$) has a Mulliken population of 7 and an isolated hydrogen ($1s^1$) has a Mulliken population of 1 . So, Ammonia has a Mulliken population of 8 . The charge transfer in terms of Mulliken population is reported in Table 2 for all four cases of having NH_3 molecule near the BN sheet surface.

The above analysis confirms that the charge transfer occurs from ammonia (NH_3) to BN sheet measured in terms of Mulliken population. During the charge transfer, the $2s$ and $2p$ orbitals of nitrogen and the $1s$ orbital of hydrogen of ammonia lost its charge to the $2s$ and $2p$ orbitals of boron and $2s$ and $2p$ orbitals of nitrogen of the BN sheet. In the case of NH_3 at bridgesite and NH_3 at boron, a charge transfer of 0.048 occurs. This may be due to the interaction between the electropositive boron and electronegative nitrogen and hydrogen, as the ammonia is placed relatively closer to a boron atom of the BN sheet. In another case of having NH_3 at the center, the charge transfer of 0.009 occurs. Here the ammonia molecule is placed in a position such that it is at the center of the BN ring. In another site, where NH_3 is sited just above the nitrogen atom of BN sheet, a small charge of 0.008 transfers. This reduction in charge transfer may be due to the lesser interaction of electronegative ammonia with the electronegative nitrogen, as the ammonia molecule is placed relatively closer to the nitrogen atom of the BN sheet.

Conclusions

The present paper discusses the NH_3 sensing behavior of BN sheet, through variations in electronic and transport properties of BN sheet; where, the band gap of BN sheet increases on introduction of the NH_3 molecule. The analysis also observed the effect of change in geometries of the NH_3 molecule present on the BN sheet; however, it shows no change in the band gap. In another analysis, different NH_3 sites have been analyzed and the bridge site found to be the most favorable adsorption site and the mechanism of interaction falls between weak electrostatic interaction and chemisorption. As a confirmation of this finding, the transport properties computation shows an increase in the transmission of electrons on increasing the bias voltage and through I-V relationship, the current increases on applying the bias when ammonia is introduced while a very small current flows for pristine BN sheet. Charge transfer analysis has also been made to understand the sensitivity of the BN sheet surface discussed in terms of Mulliken population.

Acknowledgments The authors are extremely grateful to Atal Bihari Vajpayee-Indian Institute of Information Technology and Management, Gwalior (ABV-IIITM) for providing the infrastructural support to the research work. We are also thankful to Dr. Shazad Khan, Post-Doctoral Fellow at ABV-IIITM for scientific discussion.

References

- Novoselov KS, Geim AK, Morozov SV, Jiang D, Zhang Y, Dubonos SV, Grigorieva IV, Firsov AA (2004) Electric field effect in atomically thin carbon films. *Sci Mag* 306:666–669

2. Novoselov KS, Geim AK (2007) The rise of graphene. *Nat Mater* 6: 183–191
3. Lu G, Ocula EL, Chen J (2009) Gas detection using low-temperature reduced graphene oxide sheets. *Appl Phys Lett* 94:083111
4. Pashangpour M, Bagheri Z, Ghaffari V (2013) A comparison of electronic transport properties of graphene with hexagonal boron nitride substrate and graphene, a first principle study. *Euro Phys J B* 86:269
5. Robinson JT, Perkins FK, Snow ES, Wei ZQ, Sheehan PE (2008) NO₂ and humidity sensing characteristics of few-layer graphene. *Nano Lett* 8:3137
6. Yoon HJ, Jun DH, Yang JH, Zhou Z, Yang SS, Cheng MM (2011) Carbon dioxide gas sensor using a graphene sheet. *Sens Actuators B: Chem* 157:310–331
7. Sakhavand N, Shahsavari R (2014) Synergistic behavior of tubes, junctions, and sheets imparts mechano-mutable functionality in 3D porous boron nitride nanostructures. *J Phys Chem C, Nanomater Interfaces* 118(39):22730–22738. doi:10.1021/jp5044706
8. Bhattacharya A, Bhattacharya S, Das GP (2012) Band gap functionalisation of BN sheet. *Phys Rev B* 85:035415
9. Zhang Z, Guo W, Dai Y (2009) Stability and electronic properties of small boron nitride nanotubes. *J Appl Phys* 105:084312
10. Zheng F, Zhou G, Liu Z, Wu J, Duan W, Gu BL, Zhang SB (2008) Half metallicity along the edges of zigzag boron nitride nanoribbons. *Phys Rev B* 78:205415
11. Lopez A, Bezanilla HJ, Terrones H, Sumpter BH (2012) Electronic structure calculations on edge functionalised armchair boron nitride nanoribbons. *J Phys Chem C* 116(29):15675–15681
12. Anota EC, Juarez AR, Castro M, Coccoletzi HH (2013) A density functional theory analysis for adsorption of the amine group on graphene and BN nanosheets. *J Mol Model* 19:321–328
13. Barsan N, Koziej D, Weimar U (2007) Metal oxide-based gas sensor research: how to? *Sci Direct* 121(1):18–35
14. Neek-Amal M, Beheshtian J, Sadeghi A, Michel KH, Peeters FM (2013) Boron nitride monolayer: a strain tunable nanosensor. *J Phys Chem C* 117(25):13261–13267
15. Kohl D (2001) Function and application of gas sensors, topical review. *J Phys D34*:R125–R149
16. Dubbe A (2003) Fundamentals of solid state ionic micro gas sensors. *Sensors Actuators B* 88:138–148
17. Wan Q, Li QH, Chen YJ, Wang TH, He XL, Li JP, Lin CL (2003) Fabrication and ethanol sensing characteristics of ZnO nanowire based gas sensors. *Nature* 424:171–174
18. Murray JS, Politzer P (2011) The electrostatic potential: an overview. *Comp Mol Sci* 153–163
19. Murray JS, Politzer P (2002) The fundamental nature and the role of the electrostatic potential in atoms and molecules. *Theor Chem Acc* 108:134–142
20. Banerjee S, Puri IK (2008) Enhancement in hydrogen storage in carbon nanotubes under modified conditions. *Nanotechnology* 19: 155702
21. Khan MS, Khan MS (2012) Comparative theoretical study of iron and magnesium incorporated porphyrin induced carbon nanotubes and their interaction with hydrogen molecule. *Phys E* 44:1857–1861
22. Trivedi S, Srivastava A, Kurchania R (2014) Silicene and germanene: a first principle study of electronic structure and effect of hydrogenation-passivation. *J Comput Theor Nanosci* 11(3):1–8
23. Srivastava A, Jain A, Kurchania R, Tyagi N (2012) Width dependent electronic properties of graphene nanoribbons: an ab-initio study. *J Comput Theor Nanosci* 9(7):1008–1013
24. Trivedi S, Srivastava A, Kurchania A (2014) Electronic and transport properties of silicene nanoribbons. *J Comput Theor Nanosci* 11:1–6
25. Srivastava A, Jain SK, Khare PS (2014) Ab-initio study of structural, electronic, and transport properties of zigzag GaP nanotubes. *J Mol Model* 20:2171
26. Sholl D, Steckel JA (2009) Density functional theory: a practical introduction
27. Dreizler RM, Gross EKV (1990) Density functional theory. Springer, Berlin
28. Atomistix ToolKit version 11.2.2, QuantumWise A/S (www.quantumwise.com)
29. Perdew JP, Burke K (1996) Ernzerhof M Generalized gradient approximation made simple. *Phys Rev Lett* 77:3865–3868
30. Zhang Y, Wang W (1998) Comment on Generalized gradient approximation made simple. *Phys Rev Lett* 80:890
31. Bachelet GB, Hamann DR (1982) Ernzerhof Pseudopotentials that work. *Phys Rev B* 26:4199–4228
32. Soler JM, Artacho E, Gale JD, García A, Junquera J, Ordejón P, Sánchez-Portal D (2002) The SIESTA method for ab initio order-N materials simulation. *J Phys Condens Matter* 14:2745
33. Li E, Wang X, Hou L, Zhao D, Dai Y, Wang X (2011) Study on the electronic transport properties of zigzag GaN nanotubes. *J Phys Conf Ser* 276:012046
34. Taylor J, Guo H, Wang J (2001) Ab initio modeling of quantum transport properties of molecular electronic devices. *Phys Rev B* 63:245407
35. Datta S (1995) Electronic transport in mesoscopic systems. Cambridge Univ Press, New York
36. Brandbyge M, Mozos JL, Ordejón P, Taylor J, Stokbro K (2002) Density functional method for non-equilibrium electron transport. *Phys Rev B* 65:165401